

# Photoinduced transformations of stiff-stilbene-based discrete metallacycles to metallosupramolecular polymers

*A Submission to the Proceedings of the National Academy of Science USA*

PHYSICAL SCIENCES: Chemistry

Xuzhou Yan,<sup>a,b</sup> Jiang-Fei Xu,<sup>c</sup> Timothy R. Cook,<sup>b</sup> Feihe Huang,<sup>a,1</sup> Qing-Zheng Yang,<sup>c,1</sup> Chen-Ho Tung,<sup>c</sup> and Peter, J. Stang<sup>b,1</sup>

<sup>a</sup>State Key Laboratory of Chemical Engineering, Department of Chemistry, Zhejiang University, Hangzhou, Zhejiang 310027, P. R. China

<sup>b</sup>Department of Chemistry, University of Utah, 315 South 1400 East, Room 2020, Salt Lake City, Utah 84112, United States.

<sup>c</sup>Key Laboratory of Photochemical Conversion and Optoelectronic Materials, Technical Institute of Physics and Chemistry, Chinese Academy of Sciences, Beijing 100190, P. R. China

<sup>1</sup>To whom correspondence should be addressed.

Email address: stang@chem.utah.edu; fhuang@zju.edu.cn; qzyang@mail.ipc.ac.cn

## Table of Contents (13 Pages)

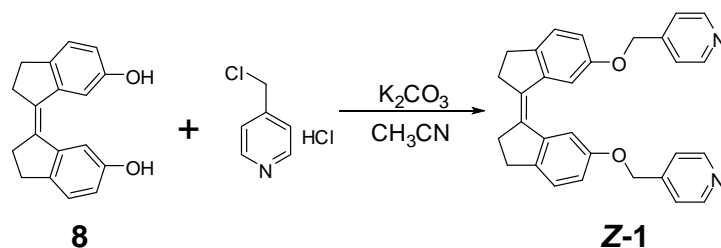
<b>Section A. Materials/General Methods/Instrumentation</b>	S2
<b>Section B. Synthetic Protocols</b>	S2
1. <i>Synthesis of stiff stilbene ligand Z-1</i>	S2
2. <i>Synthesis of stilbene-based metallacycle 4</i>	S4
3. <i>Synthesis of stilbene-based metallacycle 5</i>	S7
<b>Section C. Characterization of Metallosupramolecules</b>	S10
1. <i><sup>31</sup>P {<sup>1</sup>H} NMR spectra of DMCs 4 and 5 and MSPs 6 and 7</i>	S10
2. <i>Concentration dependence of diffusion coefficients of MSPs 6 and 7</i>	S10
3. <i>Simulated molecular models of DMCs 4 and 5</i>	S11
4. <i>Size distributions of MSPs 6 and 7 at different concentrations</i>	S11
5. <i>Partial <sup>1</sup>H NMR spectra of MSPs before and after irradiation at 360 nm</i>	S12
6. <i>Size distributions of MSPs 6 and 7 before and after irradiation at 360 nm</i>	S12
<b>Section D. References</b>	S13

## Section A. Materials/General Methods/Instrumentation

All reagents were commercially available and used as supplied without further purification. Deuterated solvents were purchased from Cambridge Isotope Laboratory (Andover, MA). Compounds **2**,<sup>S1</sup> **3**,<sup>S1</sup> and **8**<sup>S2</sup> were prepared according to the published procedures. NMR spectra were recorded with a Bruker Avance DMX 500 spectrophotometer or a Bruker Avance DMX 400 spectrophotometer with use of the deuterated solvent as the lock and the residual solvent or TMS as the internal reference. <sup>1</sup>H and <sup>13</sup>C NMR chemical shifts are reported relative to residual solvent signals, and <sup>31</sup>P{<sup>1</sup>H} NMR chemical shifts are referenced to an external unlocked sample of 85% H<sub>3</sub>PO<sub>4</sub> ( $\delta$  0.0). The two-dimensional diffusion-ordered (2D DOSY) NMR spectra were recorded on a Bruker DRX500 spectrometer. Dynamic light scattering (DLS) was carried out on a Malvern Nanosizer S instrument at room temperature. Mass spectra were recorded on a Micromass Quattro II triple-quadrupole mass spectrometer using electrospray ionization with a MassLynx operating system. UV-vis spectra were collected on a Shimadzu UV-2550 UV-vis spectrophotometer. The fluorescence experiments were conducted on a RF-5301 spectrofluorophotometer (Shimadzu Corporation, Japan). Transmission electron microscopy (TEM) investigations were carried out on a JEM-1200EX instrument. The samples for TEM experiments (Fig. 5, images A and B) were prepared by placing one drop of a dichloromethane solution of DMC **4** (or **5**) onto a carbon-coated grid. The samples for TEM experiments (Fig. 5, images C and D) were prepared by placing one drop of a dichloromethane solution of MSP **6** (or **7**) onto a carbon-coated grid. The melting points were collected on a SHPSIC WRS-2 automatic melting point apparatus.

## Section B. Synthetic Protocols

### 1. Synthesis of stiff stilbene ligand **Z-1**



*Scheme S1*

Into a 150 mL round-bottomed flask were added compound **8** (200 mg, 0.757 mmol), 4-(chloromethyl)pyridine hydrochloride (273 mg, 1.66 mmol), and  $K_2CO_3$  (1.05 g, 7.57 mmol) in 80 mL of  $CH_3CN$ . After heating at reflux under  $N_2$  for 16 h, the solvent was removed and  $CH_2Cl_2$  was added. The mixture was washed with water and brine, and then purified by flash column chromatography (dichloromethane/methanol, 100:1 v/v) to stilbene ligand **Z-1** as a yellow solid (253 mg, 75%). Mp 126.4–127.6 °C. The <sup>1</sup>H NMR spectrum of **Z-1** is shown in Figure S1. <sup>1</sup>H NMR ( $CD_2Cl_2$ , room temperature, 500 MHz)  $\delta$  (ppm): 8.40 (d,  $J = 5.5$  Hz, 4H), 7.66 (d,  $J = 2.0$  Hz, 2H), 7.18 (d,  $J = 5.5$  Hz, 4H), 7.13 (d,  $J = 8.0$  Hz, 2H), 6.70–6.75 (m, 2H), 4.97 (s, 4H), 2.80–2.88 (m, 4H), 2.70–2.773 (m, 4H). The <sup>13</sup>C NMR spectrum of **Z-1** is shown in Figure S2. <sup>13</sup>C NMR ( $CD_2Cl_2$ , room temperature, 125 MHz)  $\delta$  (ppm): 32.40, 37.88, 71.23, 112.53, 116.76, 124.06, 128.39, 138.21, 144.26, 144.32, 148.86, 152.51, and 159.29. LRESIMS is shown in Figure S3:  $m/z$  447.0  $[M + H]^+$ . HRESIMS:  $m/z$  calcd for  $[M]^+$   $C_{30}H_{26}N_2O_6$ , 446.1994; found 446.1996, error 0.4 ppm.

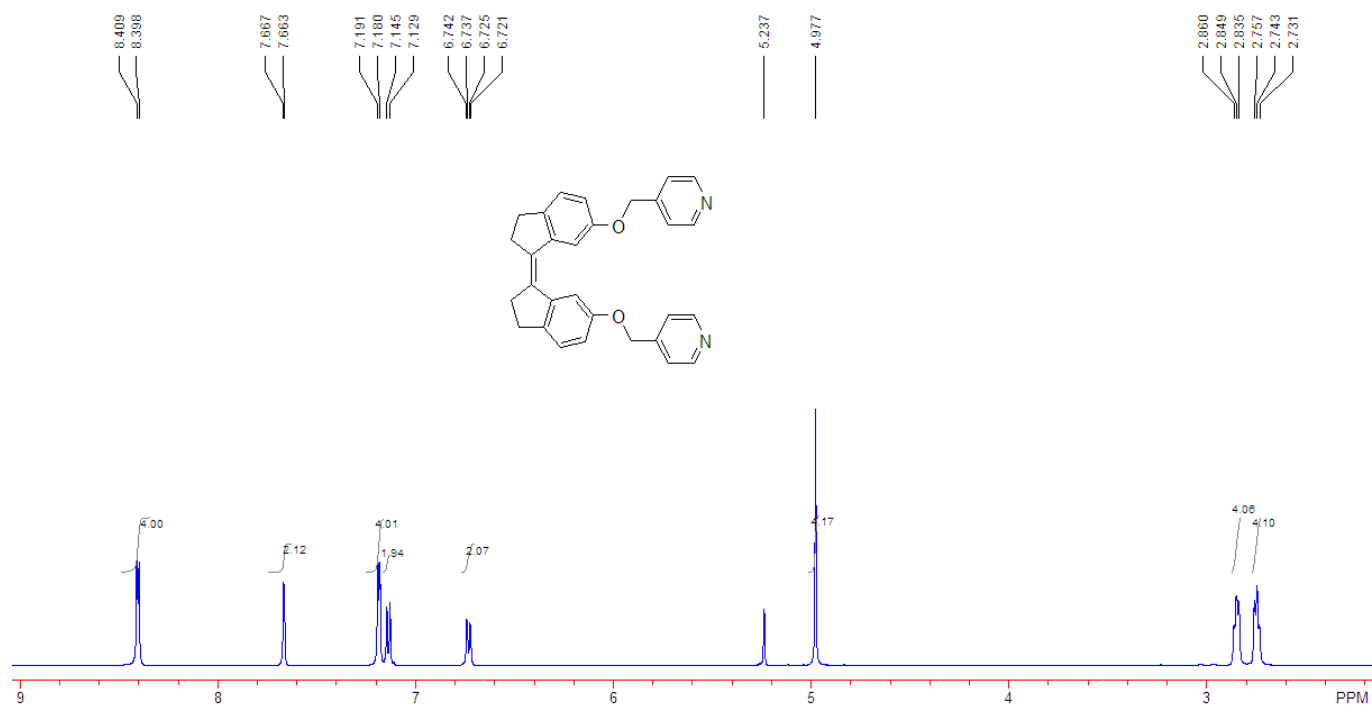


**Figure S1.** <sup>1</sup>H NMR spectrum (CD<sub>2</sub>Cl<sub>2</sub>, room temperature, 500 MHz) of Z-1.

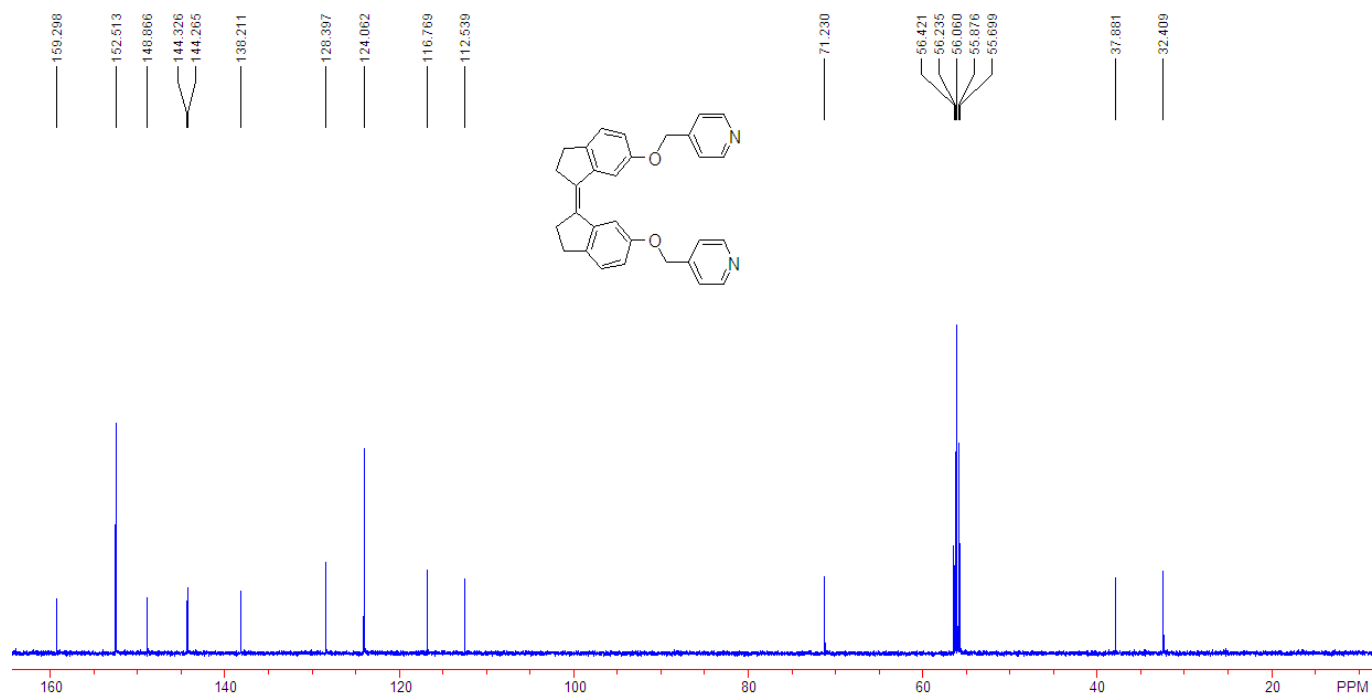


**Figure S2.** <sup>13</sup>C NMR spectrum (CD<sub>2</sub>Cl<sub>2</sub>, room temperature, 125 MHz) of Z-1.

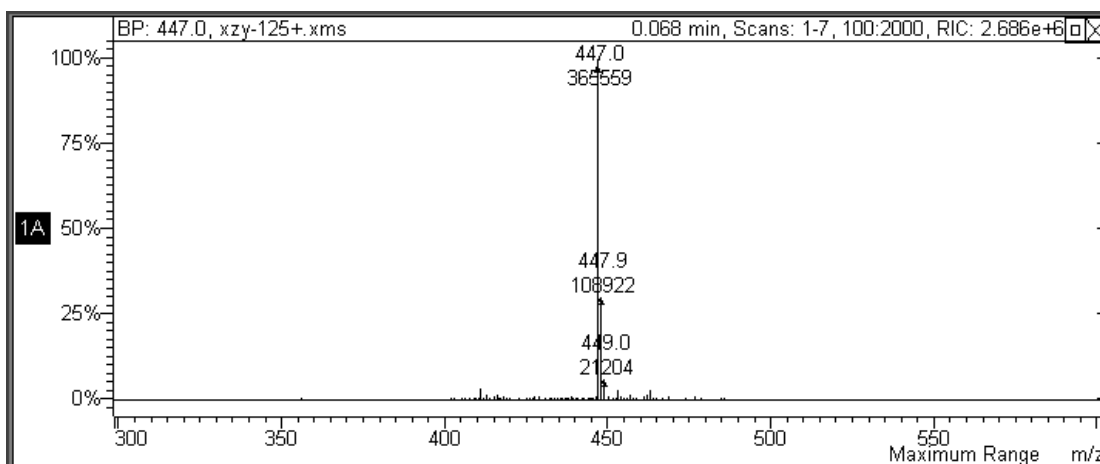
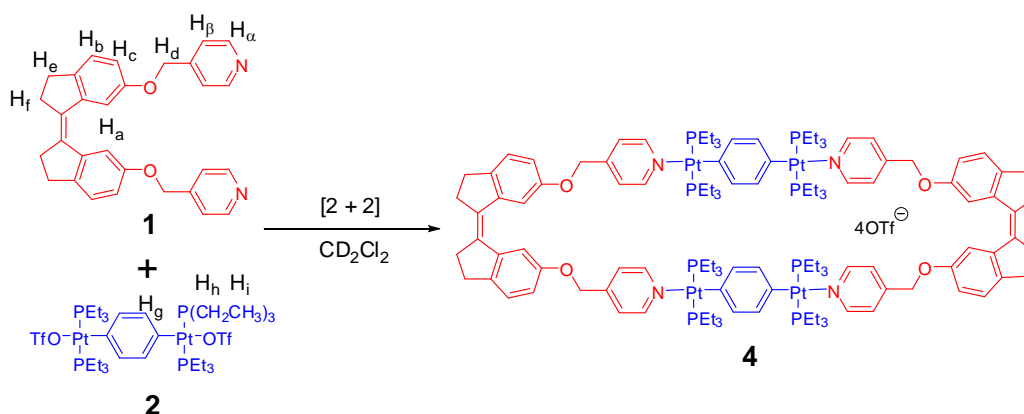


**Figure S3.** Electrospray ionization mass spectrum of **Z-1**.

## 2. Synthesis of stilbene-based metallacycle **4**



**Scheme S2**

In a 1:1 molar ratio, stiff stilbene ligand **1** (2.23 mg, 5.00  $\mu\text{mol}$ ) and 180° diplatinum acceptor **2** (6.18 mg, 5.00  $\mu\text{mol}$ ) were dissolved in 1.00 mL of  $\text{CH}_2\text{Cl}_2$  in a 2 mL dram vial. The reaction mixture was allowed to stir for 8 h at room temperature. To the resulting homogeneous solution, diethyl ether was added to precipitate the product, which was then isolated and dried under reduced pressure and re-dissolved in  $\text{CD}_2\text{Cl}_2$  for characterization. The  $^1\text{H}$  NMR spectrum of metallacycle **4** is shown in Figure S4.  $^1\text{H}$  NMR ( $\text{CD}_2\text{Cl}_2$ , room temperature, 500 MHz)  $\delta$  (ppm): 8.50 (d,  $J = 5.5$  Hz, 8H), 7.68 (d,  $J = 5.5$  Hz, 8H), 7.57 (s, 4H), 7.16 (d,  $J = 8.5$  Hz, 4H), 6.92 (s, 8H), 6.76–6.83 (m, 4H), 5.29 (s, 8H), 2.83 (t,  $J = 6.3$  Hz, 8H), 2.72 (t,  $J = 6.3$  Hz, 8H), 1.12–1.30 (m, 48H), 0.89–1.06 (m, 72H). The  $^{31}\text{P}\{^1\text{H}\}$  NMR spectrum of metallacycle **4** is shown in Figure S5.  $^{31}\text{P}\{^1\text{H}\}$  NMR ( $\text{CD}_2\text{Cl}_2$ , room temperature, 202.3 MHz)  $\delta$  (ppm): 12.79 ppm (s,  $^{195}\text{Pt}$  satellites,  $^1J_{\text{Pt-P}} = 2725.0$  Hz). ESI-MS is shown in Figure S6:  $m/z$  692.26 [ $\text{M} - 4\text{OTf}$ ] $^{4+}$ , 702.77 [ $\text{M} - 3\text{OTf} - \text{HOTf} + \text{K}$ ] $^{4+}$ , 986.67 [ $\text{M} - 2\text{OTf} - \text{HOTf} + \text{K}$ ] $^{3+}$ , 1534.47 [ $\text{M} - 2\text{OTf}$ ] $^{2+}$ , 1554.48 [ $\text{M} - \text{OTf} - \text{HOTf} + \text{K}$ ] $^{2+}$ .

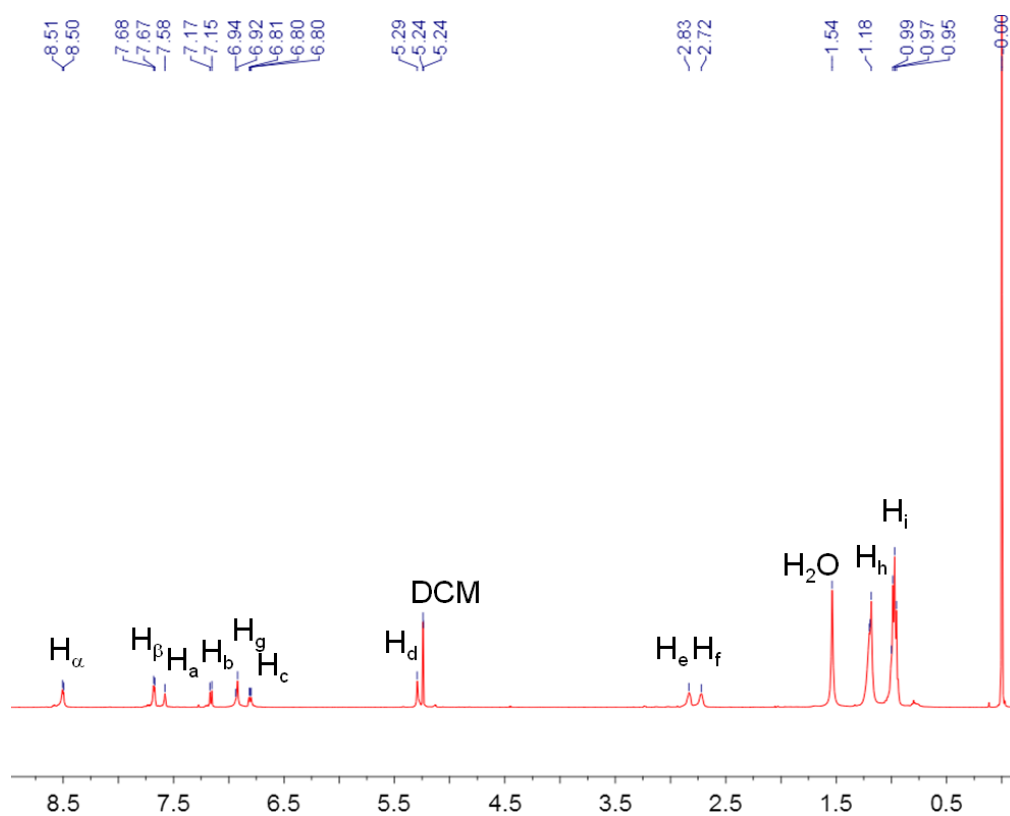


**Figure S4.**  $^1\text{H}$  NMR spectrum ( $\text{CD}_2\text{Cl}_2$ , room temperature, 500 MHz) of metallacycle **4**.

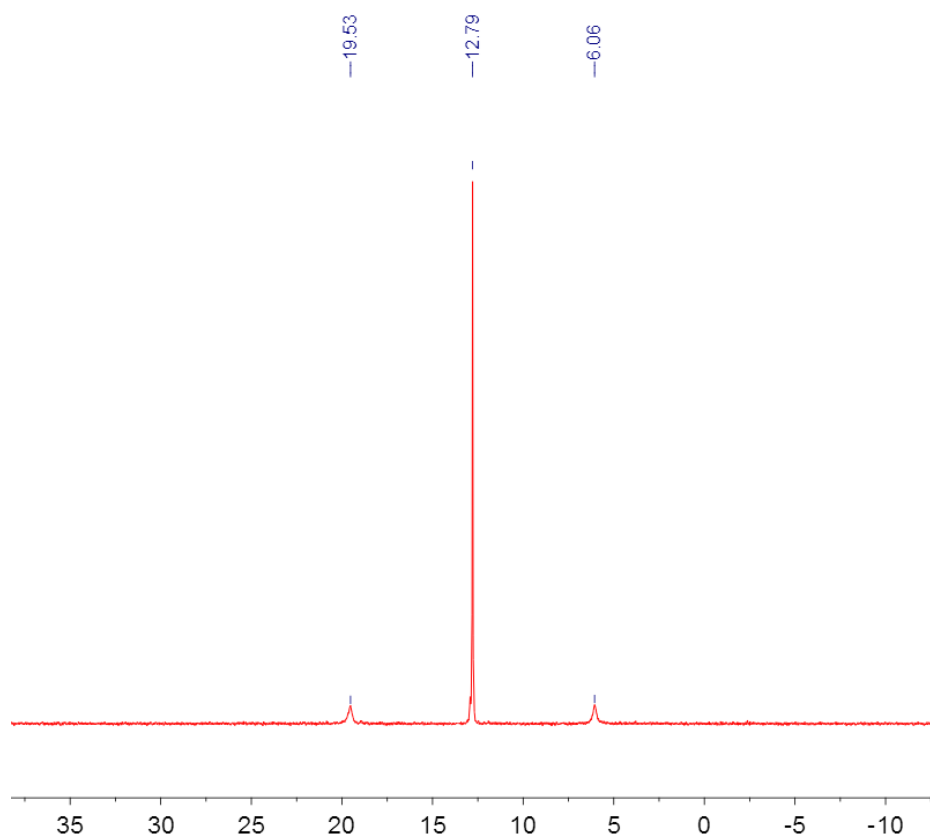


**Figure S5.**  $^{31}\text{P}$   $\{^1\text{H}\}$  NMR spectrum ( $\text{CD}_2\text{Cl}_2$ , room temperature, 202.3 MHz) of metallacycle **4**.

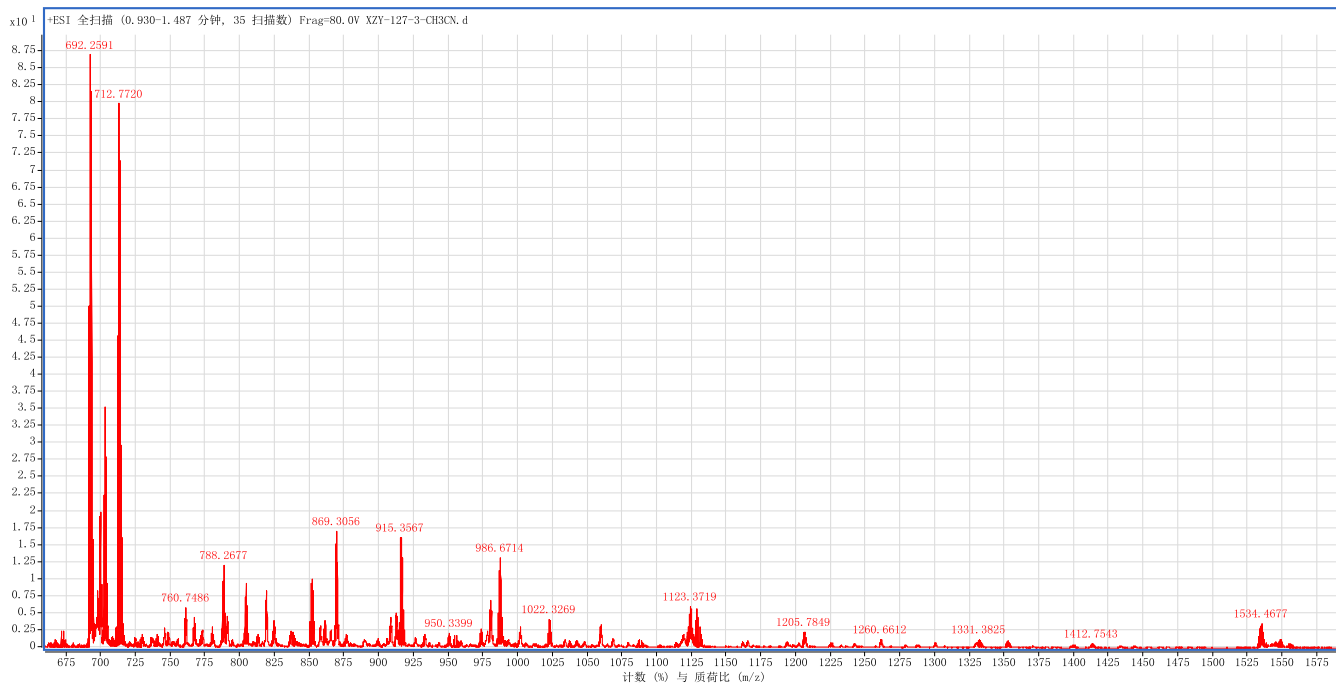
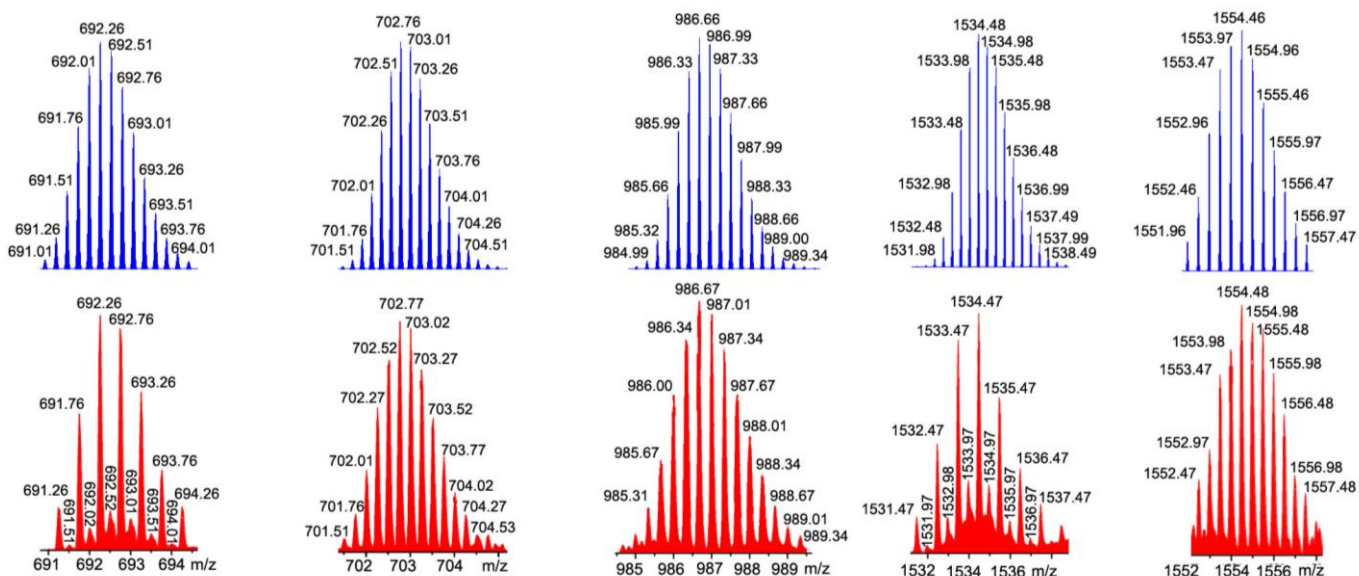
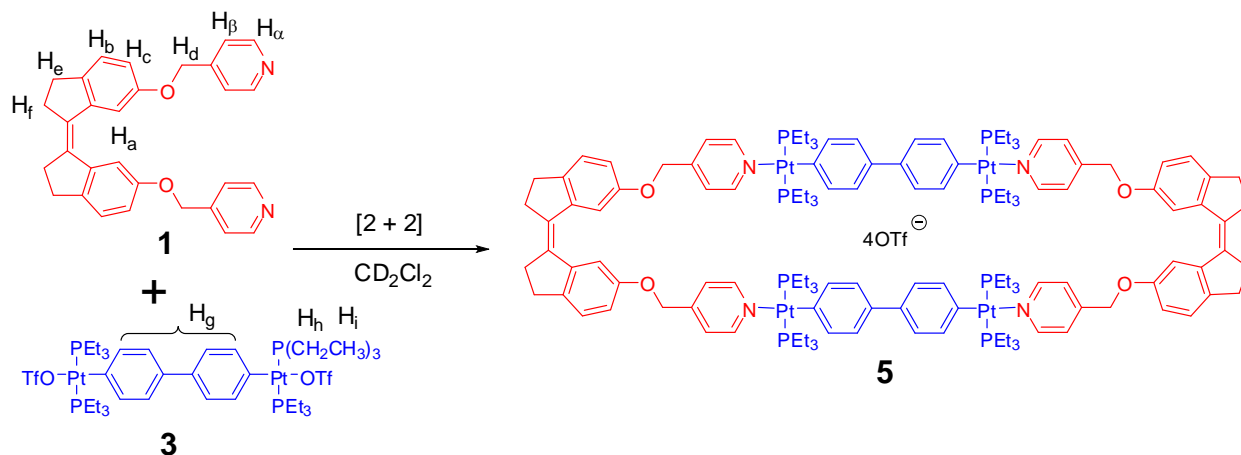


**Figure S6.** Experimental (red) and calculated (blue) electrospray ionization mass spectra of metallacycle 4.

### 3. Synthesis of stilbene-based metallacycle **5**



**Scheme S3**

In a 1:1 molar ratio, stiff stilbene ligand **1** (2.23 mg, 5.00  $\mu$ mol) and 180° diplatinum acceptor **3** (6.57 mg, 5.00  $\mu$ mol) were dissolved in 1.00 mL of  $CH_2Cl_2$  in a 2 mL dram vial. The reaction mixture was allowed to stir for 8 h at room temperature. To the resulting homogeneous solution, diethyl ether was added to precipitate the product, which was then isolated and dried under reduced pressure and re-dissolved in  $CD_2Cl_2$  for characterization. The  $^1H$  NMR spectrum of metallacycle **5** is shown in Figure S7.  $^1H$  NMR ( $CD_2Cl_2$ , room temperature, 500 MHz)  $\delta$  (ppm): 8.52 (d,  $J = 5.0$  Hz, 8H), 7.70 (d,  $J = 5.0$  Hz, 8H), 7.59 (s, 4H), 7.29 (s, 16H), 7.17 (d,  $J = 10.0$  Hz, 4H), 6.81–6.83 (m, 4H), 5.32 (s, 8H), 2.84 (t,  $J = 6.3$  Hz, 8H), 2.72 (t,  $J = 6.3$  Hz, 8H), 1.15–1.28 (m, 48H), 0.94–1.06 (m, 72H). The  $^{31}P\{^1H\}$  NMR spectrum of metallacycle **5** is shown in Figure S8.  $^{31}P\{^1H\}$  NMR ( $CD_2Cl_2$ , room temperature, 202.3 MHz)  $\delta$  (ppm): 13.49 ppm (s,  $^{195}Pt$  satellites,  $^1J_{Pt-P} = 2692.6$  Hz). ESI-MS is shown in Figure S9:  $m/z$  730.77  $[M - 4OTf]^{4+}$ , 740.78  $[M - 3OTf - HOTf + K]^{4+}$ , 1037.69  $[M - 2OTf - HOTf + K]^{3+}$ , 1610.50  $[M - 2OTf]^{2+}$ , 1630.51  $[M - OTf - HOTf + K]^{2+}$ .

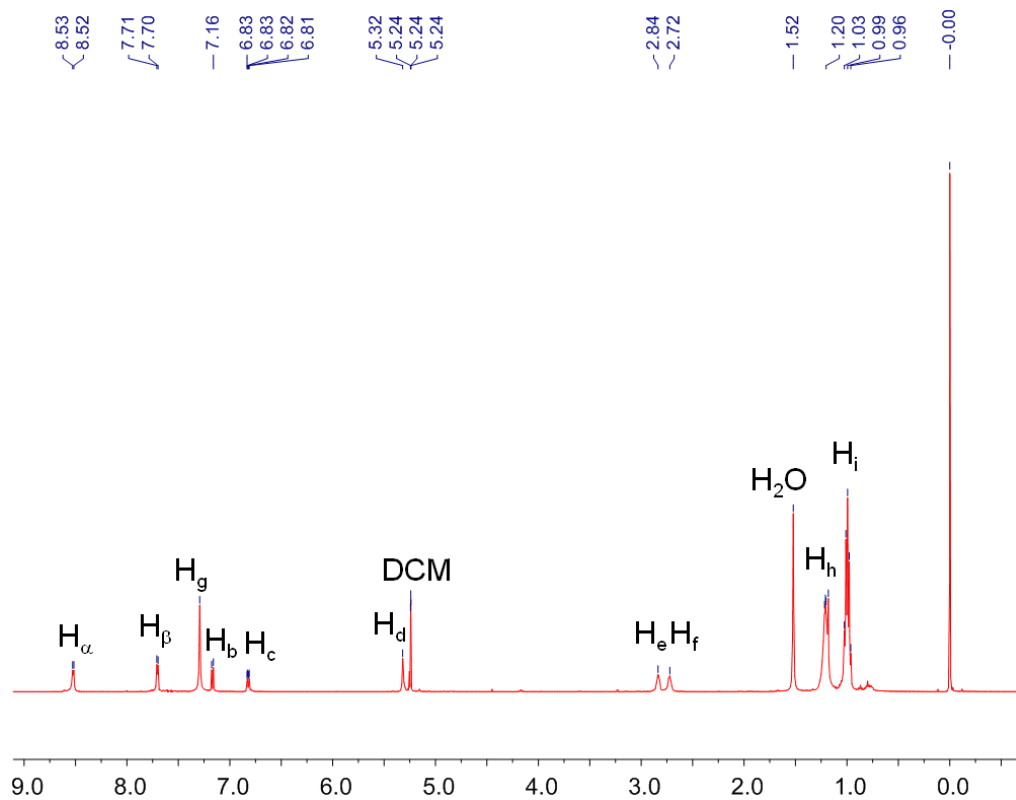


**Figure S7.**  $^1\text{H}$  NMR spectrum ( $\text{CD}_2\text{Cl}_2$ , room temperature, 500 MHz) of metallacycle **5**.

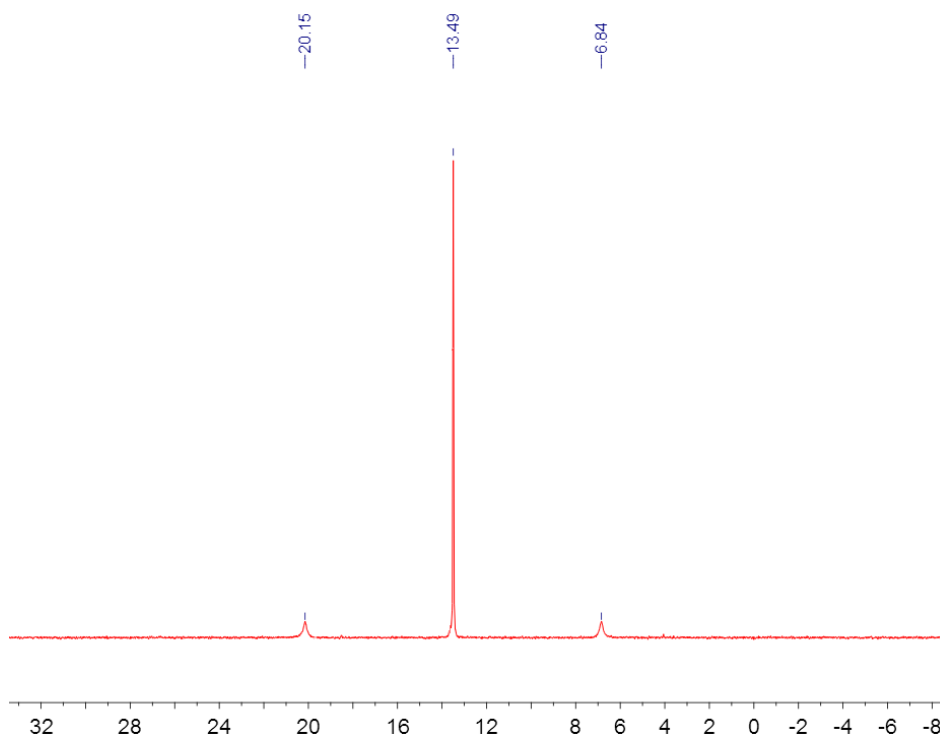


**Figure S8.**  $^{31}\text{P}$   $\{^1\text{H}\}$  NMR spectrum ( $\text{CD}_2\text{Cl}_2$ , room temperature, 202.3 MHz) of metallacycle **5**.



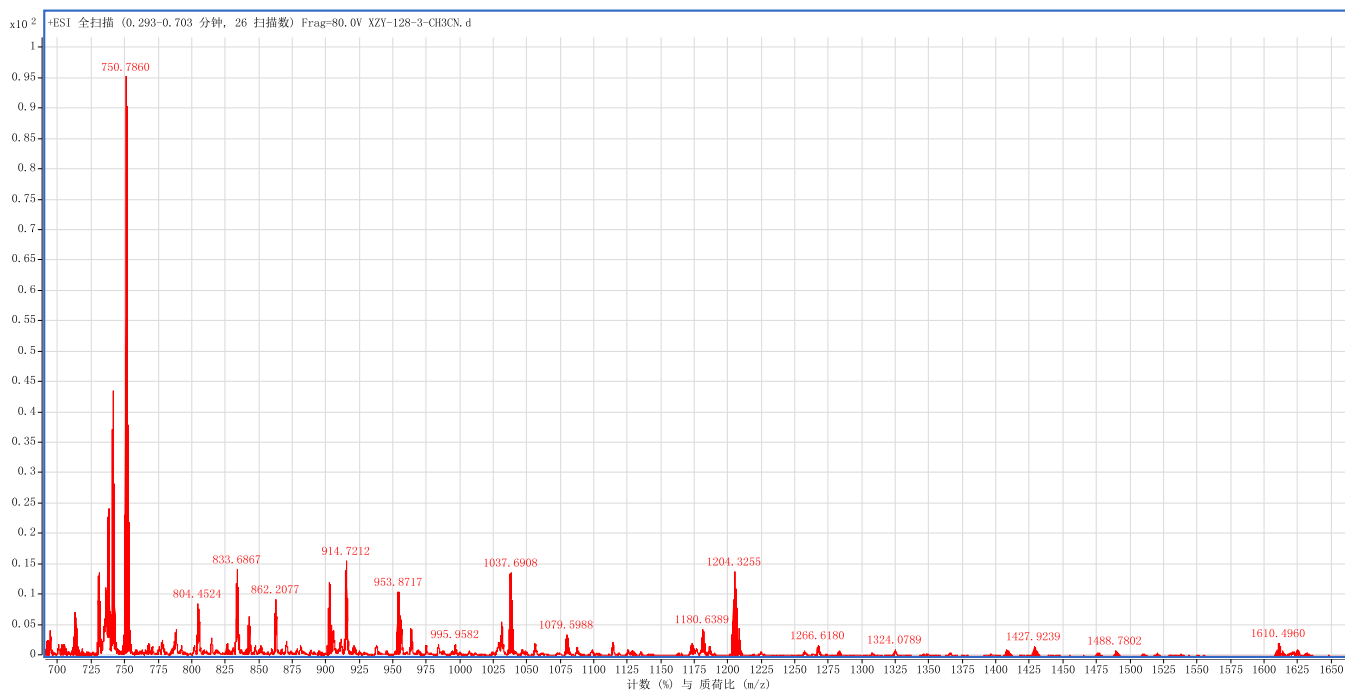
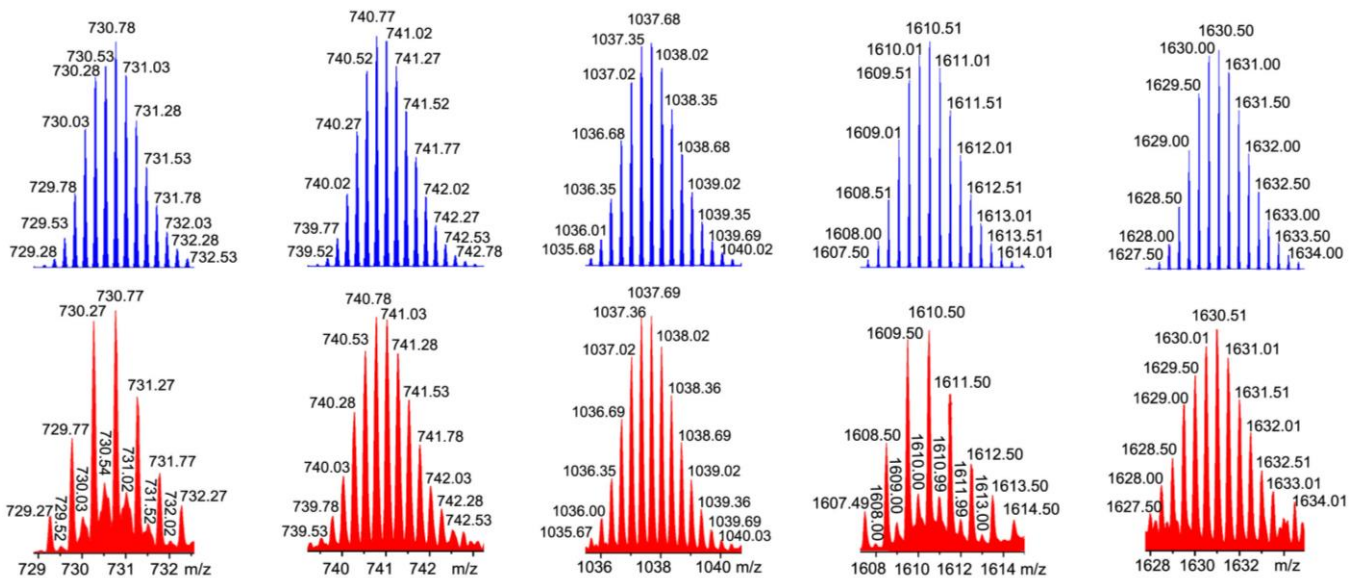


**Figure S9.** Experimental (red) and calculated (blue) electrospray ionization mass spectra of metallacycle 5.

## Section C. Characterization of Metallosupramolecules

### 1. $^{31}\text{P}\{^1\text{H}\}$ NMR spectra of DMCs **4** and **5** and MSPs **6** and **7**

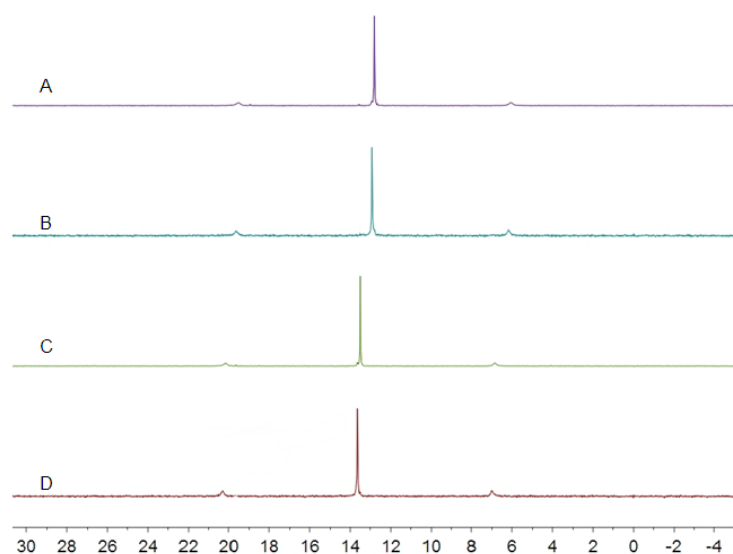


**Figure S10.**  $^{31}\text{P}\{^1\text{H}\}$  NMR spectra ( $\text{CD}_2\text{Cl}_2$ , 293 K, 500 MHz): (A) discrete metallacycle **4**; (B) metallosupramolecular polymer **6**; (C) discrete metallacycle **5**; (D) metallosupramolecular polymer **7**.  $c = 5.00$  mM.

### 2. Concentration dependence of diffusion coefficients of MSPs **6** and **7**

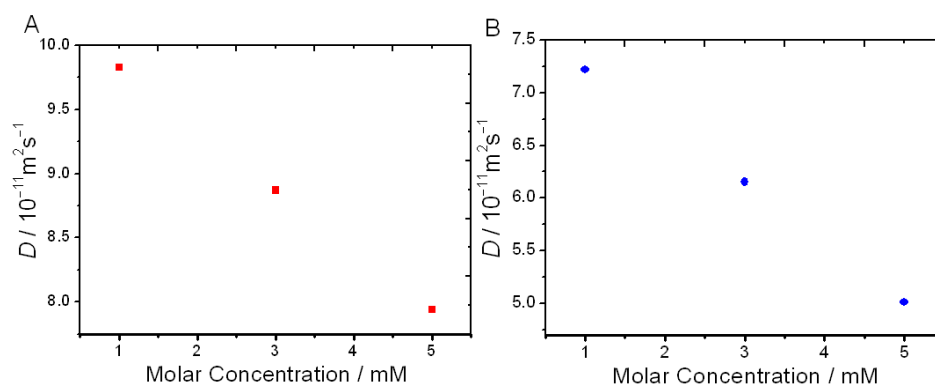


**Figure S11.** Concentration dependence of diffusion coefficients  $D$  (500 MHz,  $[\text{D}_3]\text{acetonitrile}$ , 293 K) of MSP **6** (A) and MSP **7** (B).

To further substantiate the photoinduced formation of MSPs **6** and **7**, concentration-dependent 2D DOSY experiments were performed. Upon increasing the MSPs concentration, the measured weight-average diffusion coefficients decreased from  $9.83 \times 10^{-10}$  to  $7.94 \times 10^{-10} \text{ m}^2 \text{ s}^{-1}$  for MSP **6** and  $7.21 \times 10^{-10}$  to  $5.01 \times 10^{-10} \text{ m}^2 \text{ s}^{-1}$  for MSP **7**.

### 3. Simulated molecular models of DMCs 4 and 5

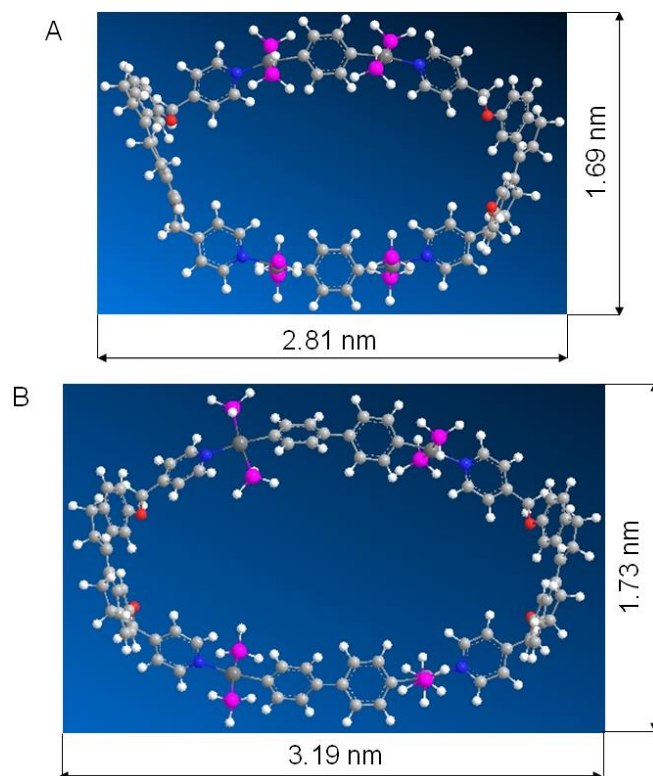


**Figure S12.** Simulated molecular models of DMCs **4** (A) and **5** (B) by PM6 semiempirical molecular orbital methods. To minimize computational cost, the  $\text{PEt}_3$  ligands were modeled as  $\text{PH}_3$ .

### 4. Size distributions of MSPs 6 and 7 at different concentrations

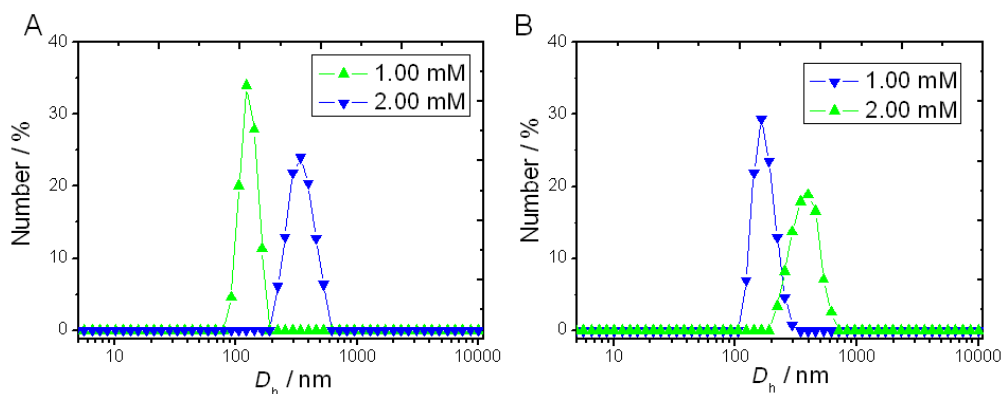


**Figure S13.** Size distributions of MSPs **6** (A) and **7** (B) at different concentrations.

5. Partial  $^1\text{H}$  NMR spectra of MSPs before and after irradiation at 360 nm

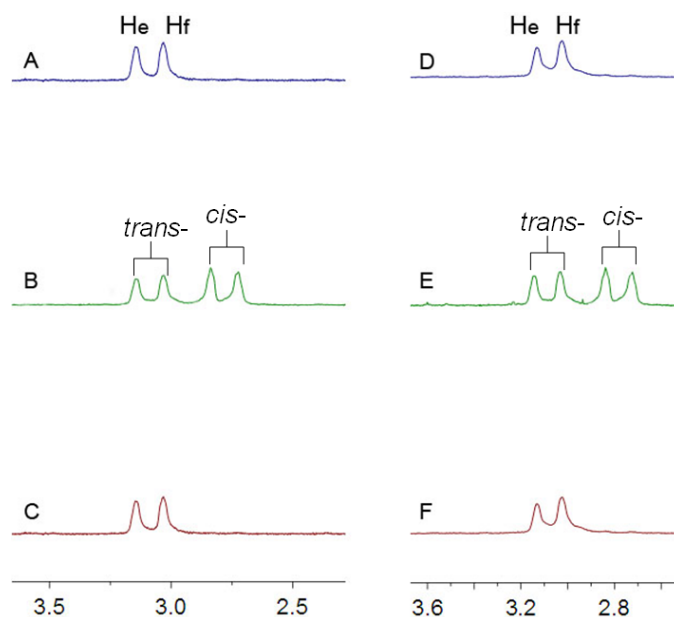


**Figure S14.** Partial  $^1\text{H}$  NMR spectra ( $\text{CD}_2\text{Cl}_2$ , 293 K, 500 MHz): (A) metallosupramolecular polymer **7**; (B) irradiation of sample (A) at 360 nm; (C) irradiation of sample (B) at 387 nm; (D) metallosupramolecular polymer **6**; (E) irradiation of sample (D) at 360 nm; (F) irradiation of sample (E) at 387 nm.  $c = 2.00$  mM.

6. Size distributions of MSPs **6** and **7** before and after irradiation at 360 nm

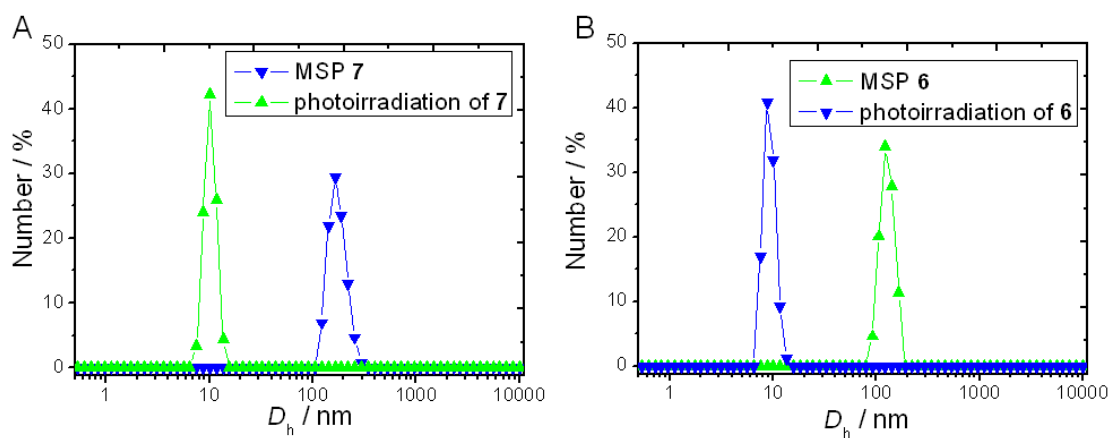


**Figure S15.** Size distributions of MSPs **7** (A) and **6** (B) before and after irradiation at 360 nm.  $c = 1.00$  mM.

## Section D. References

- S1. Manna J, et al. (1997) Nanoscale tectonics: self-assembly, characterization, and chemistry of a novel class of organoplatinum square macrocycles. *J Am Chem Soc* 119: 11611–11619.
- S2. Akbulatov S, Tian Y, Boulatov R (2012) Force–reactivity property of a single monomer is sufficient to predict the micromechanical behavior of its polymer. *J Am Chem Soc* 134: 7620–7623.